

SYNTHESIS OF HYDROGEN STORAGE MATERIALS IN A Ti-Zr-Ni SYSTEM USING THE HYDRIDE CYCLE TECHNOLOGY DURING DEHYDROGENATION BY AN ELECTRON BEAM IN A VACUUM

*O.E. Dmytrenko, V.I. Dubinko, V.M. Borysenko, K. Irwin**

National Science Center "Kharkov Institute of Physics and Technology", Kharkiv, Ukraine;

**Quantum Gravity Research, Los Angeles, CA*

E-mail: dmitrenko@kipt.kharkov.ua

The synthesis of intermetallic material was carried out by means of dehydrogenating annealing of a $(\text{TiH}_2)_{30}\text{Zr}_{45}\text{Ni}_{25}$ sample in vacuum by an electron beam. The properties of the obtained material were studied for establishing the structural phase composition by scanning electron microscopy and X-ray structural analysis. It was found that prolonged exposure of an electron beam to a sample containing titanium hydride leads to a number of structural transformations in the material, accompanied by a redistribution of hydrogen from titanium to zirconium and culminating in the synthesis of a ternary alloy with characteristic growth structures. The processes of hydrogen sorption-desorption by a synthesized sample were studied, the temperature ranges of these processes and the absorption capacity of the obtained material were established. It was shown that the structure of the sample formed upon heating by an electron beam promotes the absorption of hydrogen at room temperature up to 1.41 wt. %.

INTRODUCTION

The possibility of synthesizing complex intermetallic and quasicrystalline materials based on refractory metals of the zirconium group using hydride technology was shown in [1–8]. These materials are capable of reversibly absorbing hydrogen in significant quantities over 2 wt. % [9–11], which allows us to consider them as materials for the storage of hydrogen. The studies conducted earlier [12, 13] showed that materials of the Ti-Zr-Ni system obtained by the rapid quenching method and containing the Laves phase C14 (L-TiZrNi) absorb hydrogen in the temperature range 450...550 °C. The maximum amount of hydrogen when saturated from the gas phase occurs at 450 °C and is characterized by slow sorption to values of about 1.8 wt. %. For the industrial use of these materials as hydrogen storage devices, it is necessary to increase the absorption coefficient and reduce the sorption-desorption temperatures. In addition, the synthesis of samples by spinning is inefficient and technically complex, requires the use of expensive vacuum equipment. Therefore, it is necessary to develop more productive techniques that allow the synthesis of bulk samples with a given structure and properties. In this work, we studied the structure and properties of the $(\text{TiH}_2)_{30}\text{Zr}_{45}\text{Ni}_{25}$ sample during its layer-by-layer dehydrogenation in a vacuum under the influence of an electron beam. The technology of the "hydride cycle", based on the interaction of the decomposition products (dissociation) of the hydrides of the initial components with the formation of systems and phases characteristic of these materials with significantly less energy consumption. Hydrogen, in this case, plays the role of a temporary alloying impurity to titanium and zirconium, leaving the sample when heated in a vacuum, but having a positive effect on the process of converting the system of starting dispersed particles into a massive (consolidated) alloy. Titanium and zirconium, as elements of one group of the periodic system, have similar characteristics of interaction with hydrogen, in

particular, they have similar binary phase diagrams with hydrogen (both metals form hydrides). Dehydrogenation with an electron beam will allow gradient heating of the sample and, therefore, obtain a sample with all intermediate structural states from hydride to ternary alloy. And, therefore, with a cross-section, it will allow studying/observe these processes of structural transformations, which in turn will expand the possibilities of synthesis of materials of the Ti-Zr-Ni system with predetermined properties.

MATERIALS AND METHODS

To prepare the sample $(\text{TiH}_2)_{30}\text{Zr}_{45}\text{Ni}_{25}$ (wt. %), the powders of the starting components were used: TiH_2 (with a hydrogen content of 3.8 wt. %, Zr powder (ПЦПК-1) Ni powder (ПНЭ-1)). The powders were mixed by grinding in an alundum mortar for 10 min. The resulting mixture powders were pressed into a briquette of \varnothing 30 mm and a height of 15 mm with a load of 77 t.

Annealing/dehydrogenation of the sample was carried out by an electron beam in a high vacuum at the EBM-1 facility [14]. Electron beam treatment of the sample $(\text{TiH}_2)_{30}\text{Zr}_{45}\text{Ni}_{25}$ was carried out in vacuum $(1...5) \cdot 10^{-2}$ Pa. The structure and composition of the samples were studied by scanning electron microscopy (SEM) and X-ray energy-dispersive microanalysis (EDX), using a SEM JSM 7001F with an accelerating voltage of 20 kV. Observation of the structure was carried out both in the secondary electron (SEI) mode and in the backscattered electron (COMPO) mode forming the composite image contrast. The composition was analyzed using the INCA PentaFET*3 detector and the Oxford Instruments INCA 4.11 program. Diffractometric studies of the samples were carried out on a DRON-4-07 X-ray diffractometer in copper $\text{Cu-K}\alpha$ radiation using a selectively absorbing β -filter. Diffracted radiation was recorded by a scintillation detector. The diffraction patterns were taken in step mode. The following samples of composition $(\text{TiH}_2)_{30}\text{Zr}_{45}\text{Ni}_{25}$ were taken for research: a) the melted

part; b) not melted part. The samples were saturated with hydrogen from the gas phase in two different chambers: a) a metal chamber with a vacuum pumping system and a hydrogen/deuterium supply system with a pressure of up to 3 atm; b) in an installation with an MX7203 mass spectrometer at a hydrogen pressure of 10 mm Hg and heating in the range of 20...450 °C for 3 h. The temperature increased at a rate of 5 °C/min in a hydrogen atmosphere. The temperature difference at the boundaries of the heat treatment region is ± 20 °C. The cooling of the furnace to 20 °C took place in a hydrogen atmosphere. Hydrogen-saturated samples of Ti-Zr-Ni alloys were investigated for desorption by heating in a vacuum in the temperature range 0...900 °C using a setup with an MX7203 mass spectrometer. The MX7203 mass spectrometer is designed to determine the hydrogen in the alloys and the composition of the gas phase released from the material when heated in a vacuum.

RESULTS AND DISCUSSION

The sample obtained after electron beam melting was partially melted: the upper part of the briquette was melted to a depth of 4 mm. The rest of the briquette is not fused, it easily crumbles with little effort. For analysis of XRD, the upper (melted) and lower (non-melted) parts of the sample were taken, which were mechanically fragmented into several parts (the resulting sample is extremely fragile and easily collapses upon impact). For SEM/EDX studies, a transverse kink of the sample was used, thus the structure from the molten surface to the unsintered powders was analyzed. Electron microscopy showed that there is a significant structural heterogeneity along with the depth of the sample.

Under the influence of an electron beam, the gradual heating of the sample begins. Since the sample is located on a copper water-cooled crystallizer, and the electron beams are focused on the upper surface of the sample, a heat gradient arises from the top-down of the sample. With further heating of the upper surface and reaching the dissociation temperature of titanium hydride, the process of sequential decomposition of TiH_2 begins according to the scheme [15]: $\text{TiH}_2(\epsilon) \rightarrow \text{TiH}_2(\delta) \rightarrow \text{Ti}(\beta) \rightarrow \text{Ti}(\alpha)$. However, as it was established during a preliminary study of the thermal desorption of TiH_2 shown in Fig. 1, the active decomposition of titanium hydride occurs at a temperature of 500...550 °C, at the same time, at this temperature, zirconium powder actively absorbs hydrogen, since the decomposition temperature of ZrH_2 is higher than that of TiH_2 at 100...150 °C (see Fig. 1).

Thus, the heating of the $(\text{TiH}_2)_{30}\text{Zr}_{45}\text{Ni}_{25}$ sample by an electron beam is accompanied by a series of structural transformations that occur during the redistribution of hydrogen from TiH_2 to ZrH_2 and the subsequent decomposition of $\text{ZrH}_2(\epsilon) \rightarrow \text{ZrH}_2(\delta) \rightarrow \text{Zr}(\beta) \rightarrow \text{Zr}(\alpha)$ with increasing temperature [16]. Since the beam power is set necessary for slow heating of the sample and does not change further, a stationary dehydrogenation process is established in the chamber

in which the above transformations occur layer by layer, as the sample is heated from top to bottom. During dissociation during annealing in vacuum, TiH_2 and ZrH_2 emit hydrogen, gradually turning into metals, and a decrease in the concentration of hydrogen in their crystal lattices leads to a sequence of phase transformations. Due to the presence of bonds broken during dissociation, the obtained metal titanium and zirconium actively interact with each other and with nickel at temperatures well below their melting points. An additional factor contributing to the interaction is the cleaning of the surfaces of the powders from oxide films by active hydrogen released during the decomposition of hydrides, as shown in [17].

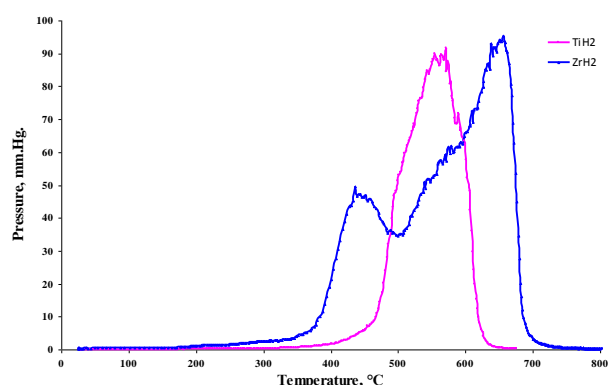


Fig. 1. Thermal desorption TiH_2 and ZrH_2

The fusion process begins with the local melting of individual Ti, Zr, Ni particles at the contact boundary with the formation of the eutectic (Fig. 2,a). As the sample is heated and the temperature rises in volume, the local boundary fusion passes into the melt zones with the involvement of a larger number of initial components. The resulting eutectic type melt (since a composition close to the eutectic is taken) penetrates deep into the sample, the melt zone expands (see Fig. 2,b). When an equilibrium annealing process is established (all heat transferred to the upper part of the sample by an electron beam is removed through the lower part of the sample located on a copper water-cooled tray), a new/gradual formation of a new structure in the melt zone occurs.

At a certain point in time (at a certain temperature, composition, temperature gradient), more refractory crystallization centers form in the melt (see Fig. 2,c). Since this composition of the Ti-Zr-Ni melt corresponds to eutectic, and the temperature at the beginning of crystallization, we obtain a mixture of more refractory crystals, presumably enriched with zirconium, surrounded by more fusible melts with a high content of titanium and nickel (see Fig. 2,d). This was confirmed by the EDX analysis data presented in Table. The Zr content in the growth structures is 56 wt.%, in contrast to 43...45 wt.% in the eutectic matrix surrounding them. Classical eutectic precipitation will not occur since the sample continues to be heated by the electron beam and the melt zone continues to propagate down the sample.

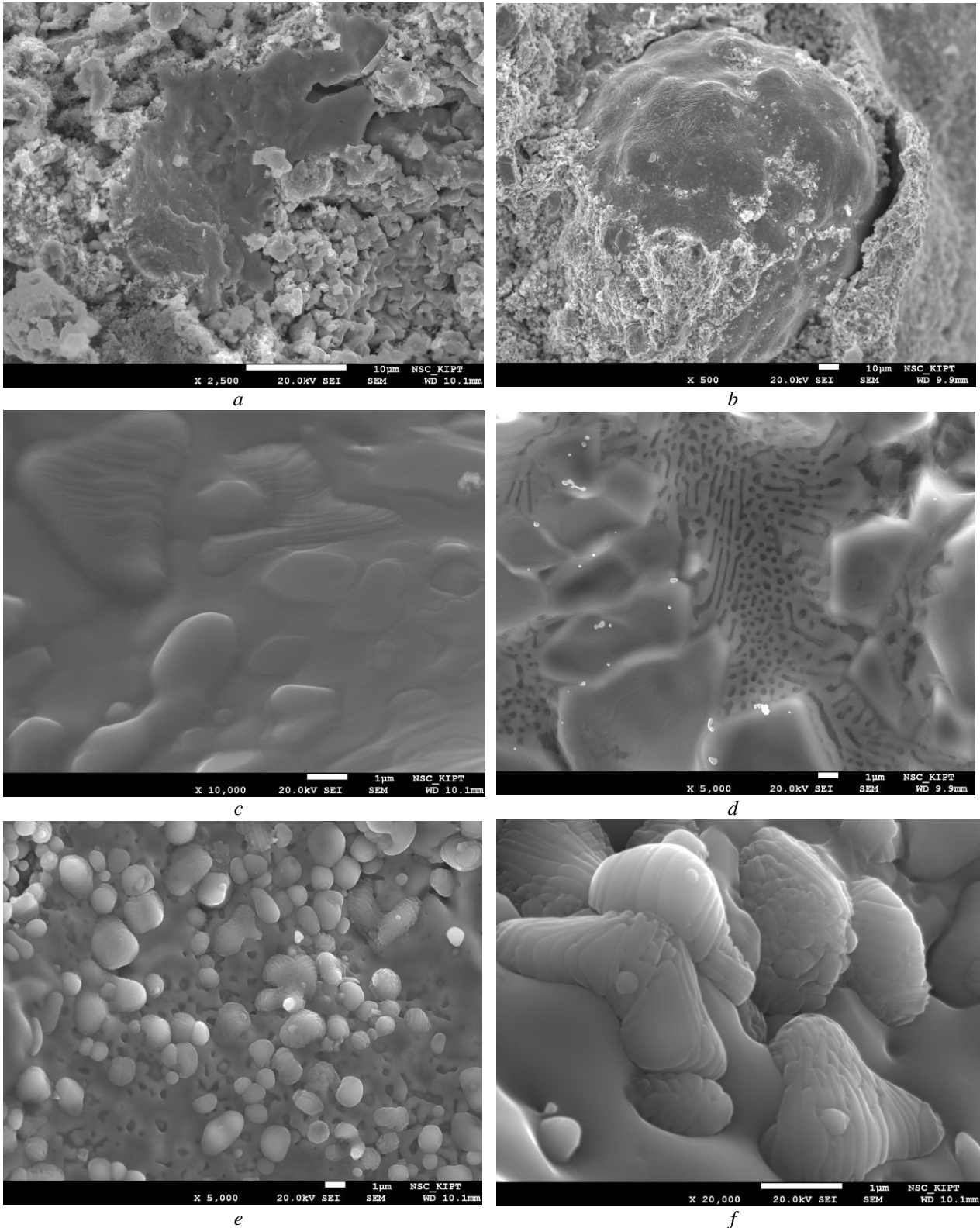


Fig. 2. Formation of growth patterns characteristic of the given system with gradual melting of the sample

After the equilibrium process is established, with a constant beam power that corresponds to the melting point of the eutectic and a constant heat removal rate, i.e., we have a constant temperature gradient, the melt and crystallization centers create optimal conditions for polycrystalline grain growth. As can be seen from Fig. 2,e,f the growth patterns characteristic of this system are formed. As these formations grow, the amount of surrounding eutectic decreases accordingly.

At a distance of less than 1 mm from the heated upper surface of the sample, the crystals completely “absorb” the surrounding eutectic and grow to the maximum size limited by neighboring formations. Considering the duration of the annealing process (about 3 h), significant formations up to 500 µm in size are formed (Fig. 3).

Since the gradual melting of the sample occurs, all of the above processes occur in layers as the sample is melted, i.e. simultaneously: in a layer located 3 mm

from the upper part of the sample, crystallization centers surrounded by a eutectic only appear (see Fig. 2,c,d); in a layer of 2 mm (from the upper part of the sample) crystalline multilayer formations (growth figures) have already formed, partially surrounded by a eutectic (see Fig. 2,e,f); in a 1 mm layer, crystals completely absorbing the surrounding eutectic, grow to maximum

sizes (limited by adjacent formations) form spherical formations consisting of square pyramids and octahedra (see Fig. 3,a,b); on the surface of the sample (directly under the electron beam) the previously formed spherical formations begin to melt due to the gradual heating of the entire sample (see Fig. 3,c,d).

Data from EDX analysis of growth patterns and surrounding eutectics

Element	Ti K	Ni K	Zr L	Hf L	Totals
Growth patterns	21.73	19.41	56.66	2.20	100.00
Surrounding matrix	31.70	26.07	42.23	—	100.00

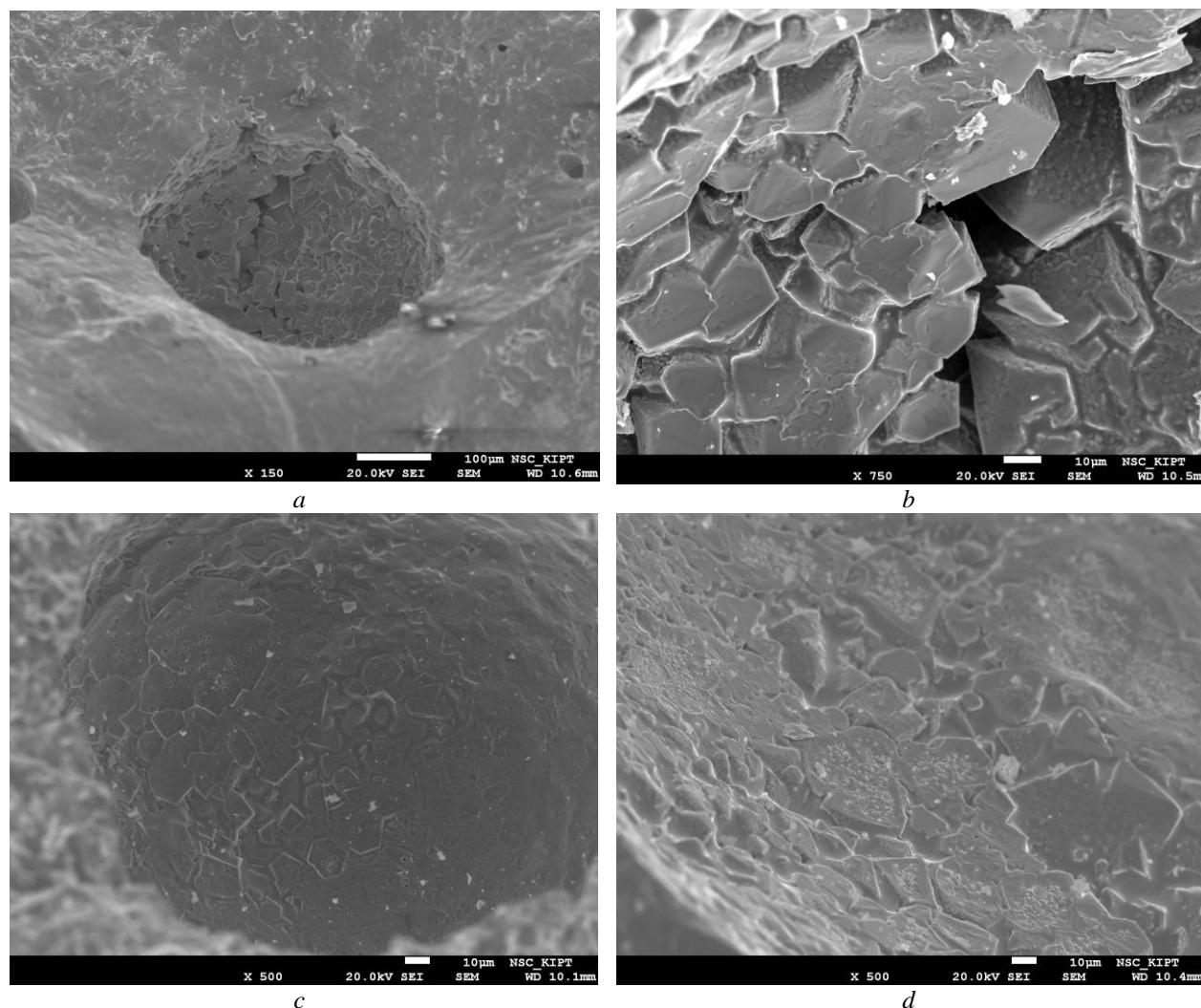


Fig. 3. Spherical formations consisting of square pyramids and octahedrons (a, b); reflow of previously formed spherical formations consisting of square pyramids and octahedrons (c, d)

Thus, the obtained sample contains various structural elements that are formed during the long-term exposure of the initial sample $(\text{TiH}_2)_{30}\text{Zr}_{45}\text{Ni}_{25}$ electron beam. The stages characteristic for each stage can be distinguished: fusion of the initial components Ti, Zr, Ni \rightarrow formation of growth structures surrounded by eutectics \rightarrow conglomerates of square pyramids \rightarrow fusion of previously formed square pyramids and octahedrons. An additional factor for the formation of structural features in this sample is the dissociation of titanium hydride into hydrogen and titanium. And

accordingly, the active diffusion of released hydrogen in a sample heated to a pre-melting temperature.

PHASE ANALYSIS OF SAMPLES $\text{Ti}_{30}\text{Zr}_{45}\text{Ni}_{25}$

X-ray diffraction patterns of the samples are shown in Fig. 4. The results of studies of the phase composition of the samples showed that 4 phases were identified in the melted upper part of the sample (see Fig. 4,a): $(\text{Ti,Zr})_2\text{Ni}$, Laves phase L-TiZrNi , $\text{Ti-}\alpha$, and $\text{Zr-}\alpha$. The lattice parameter of the $(\text{Ti,Zr})_2\text{Ni}$ phase is $a = 11.761 \text{ \AA}$. The lattice parameters of the Laves phase are $a = 5.222 \text{ \AA}$; $c = 8.558 \text{ \AA}$. The lattice parameters of titanium are $a = 2.964 \text{ \AA}$; $c = 4.618 \text{ \AA}$. The lattice

parameters of zirconium are $a = 3.242 \text{ \AA}$; $c = 5.156 \text{ \AA}$. Due to the superposition of some diffraction lines on each other, some phases are not identified, including the quasicrystalline phase.

The presence of three phases was revealed in the unmelted lower part of the sample (see Fig. 4,b): tetragonal zirconium hydride $\epsilon\text{-ZrH}_{2-x}$, cubic titanium hydride TiH_2 , and nickel Ni. The lattice parameters of the $\epsilon\text{-ZrH}_{2-x}$ phase are: $a = 3.496 \text{ \AA}$; $c = 4.493 \text{ \AA}$. The lattice parameter of titanium hydride TiH_2 is $a = 4.411 \text{ \AA}$. The lattice parameter of nickel Ni is $a = 3.524 \text{ \AA}$. In addition, the sample contains diffraction lines that could not be indicated.

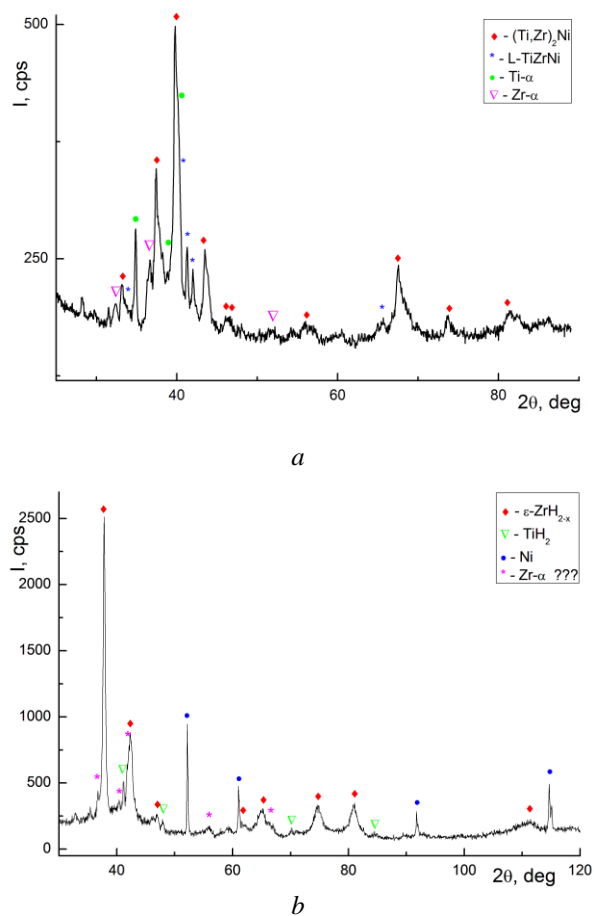


Fig. 4. Diffraction pattern of the sample $(\text{TiH}_2)_{30}\text{Zr}_{45}\text{Ni}_{25}$: upper melted part (a); lower not melted part (b)

Since there was no zirconium hydride in the initial sample, therefore, the presence of $\text{ZrH}_2(\delta)$ in the lower non-melted part of the sample confirms that the hydrogen formed during the decomposition of titanium hydride is absorbed by zirconium. And only then, with a further increase in temperature, does the sample leave. The presence in the sample of unusual structural formations shown in Figs. 2, 3 gave a prerequisite for research on the interaction of this material with hydrogen.

THE STUDY OF SORPTION-DESORPTION

For conducting research, a sample of the upper molten portion weighing 2.8 g was previously ground by grinding in an alundum mortar. Grinding was carried

out immediately before the experiment. After loading the sample into the reaction chamber, the chamber was evacuated to a pressure of $5 \cdot 10^{-6}$ bar. After the evacuation, hydrogen was introduced into the reaction chamber. The initial hydrogen pressure in the reaction chamber was 198 kPa. About 500 s after the hydrogen was introduced into the reaction chamber, intense heat evolution began, which led to an increase in the temperature of the sample (Fig. 5,a). The rate of heat evolution was proportional to the rate of change in pressure in the reaction chamber Fig. 5,b. The heat was generated by pulses. The heat generation impulsivity is especially pronounced at the initial stage of hydrogen absorption. When saturated, the sample absorbed about 1.41% by weight of hydrogen for 1.5 h. The relatively small amount of absorbed hydrogen can be explained by the predominance of the $(\text{Ti,Zr})_2\text{Ni}$ phase over the Laves phase of L-TiZrNi . As was established earlier [10], the absorption potential of the $(\text{Ti,Zr})_2\text{Ni}$ phase is much lower than that of the Laves phase. However, in contrast to rapidly quenched tapes of the same composition starting to absorb hydrogen when heated above $400 \text{ }^\circ\text{C}$, this sample began to absorb hydrogen at $12 \text{ }^\circ\text{C}$ after a short incubation period.

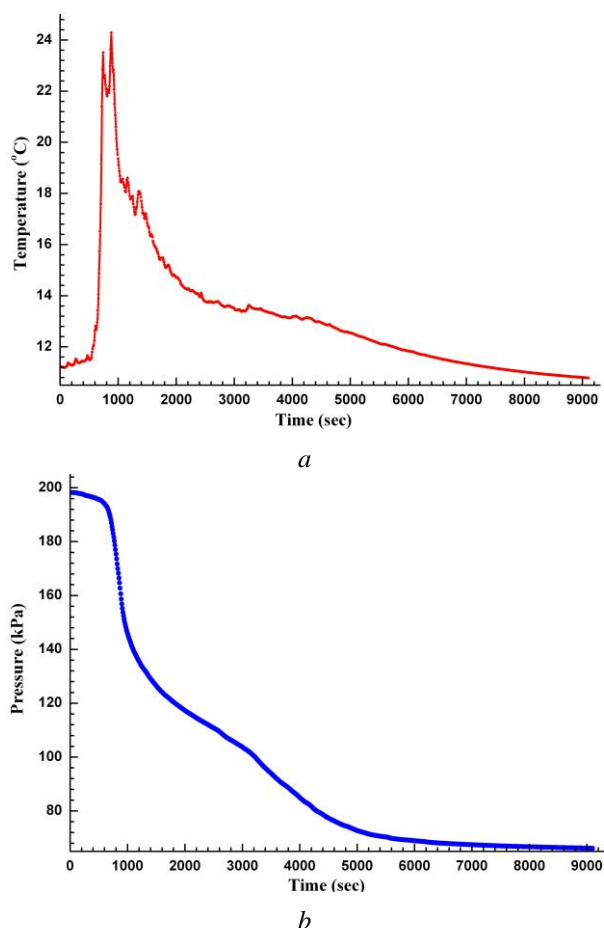
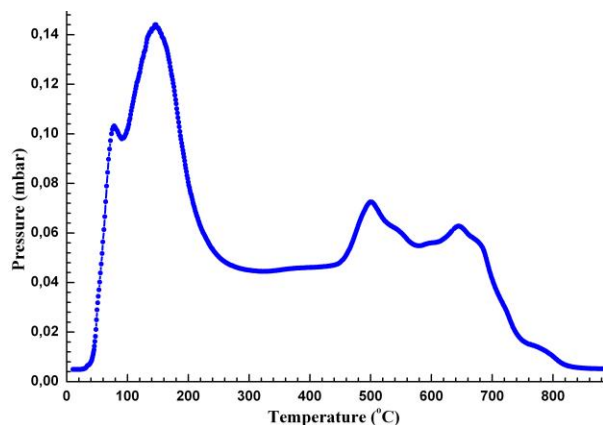


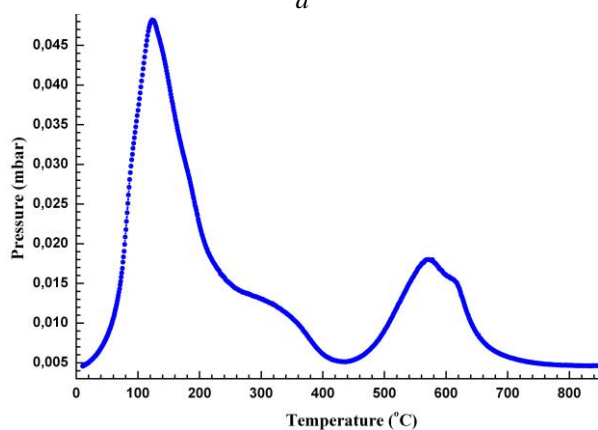
Fig. 5. Dependences of the temperature of sample (a) and the pressure in the reaction chamber (b) on time, when the $\text{Ti}_{30}\text{Zr}_{45}\text{Ni}_{25}$ sample is saturated with hydrogen at room temperature

After saturation with hydrogen at room temperature, the sample was subjected to thermal desorption by heating to $900 \text{ }^\circ\text{C}$ and cooling to room temperature with

continuous vacuum pumping. Fig. 6,a shows the dependence of the pressure in the reaction chamber on the temperature of the sample during monotonous heating of the sample at a constant rate of pumping the reaction chamber to a low vacuum after a heating cycle. Intensive gas evolution from the sample began at about 40 °C and lasted with variable intensity up to a temperature of 800 °C. The presence of several peaks of gas evolution indicates the evolution of hydrogen from various phases present in the sample, which corresponds to XRD analysis.



a

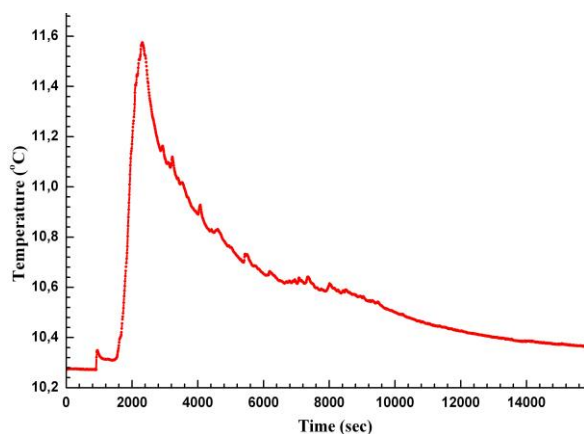


b

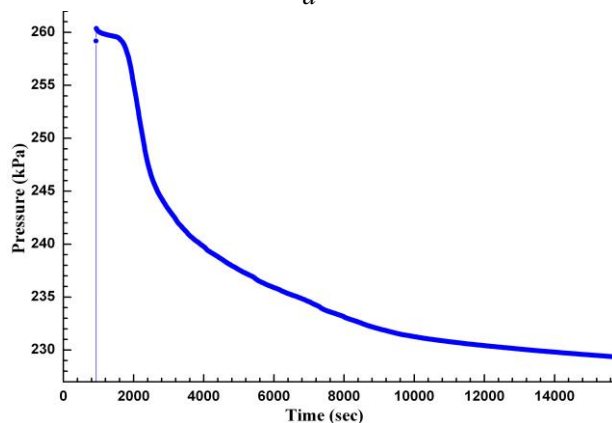
Fig. 6. The dependence of the pressure in the reaction chamber on the temperature of the sample when the sample is heated at a constant rate of evacuation of the reaction chamber to vacuum after the first saturation (a), after re-saturation (b)

After degassing, the sample was re-saturated with hydrogen at room temperature Fig. 7. The initial hydrogen pressure in the reaction chamber was 260 kPa. Upon repeated saturation, the absorption of hydrogen by the sample began with approximately the same delay as at the first saturation. The heat generation impulsivity was also observed. The intensity of the heat during the second saturation was significantly lower, but it took a longer time. The amount of heat was proportional to the magnitude of the change in pressure in the reaction chamber. Upon re-saturation, the sample absorbed 0.34 wt.% hydrogen for 4 h. Thus, it was found that this material is capable of absorbing hydrogen at room temperature after a dehydrogenation cycle. Subsequent dehydrogenation showed identical kinetics of thermal desorption (see Fig. 6,b).

The next stage of studies on the interaction with hydrogen was carried out on the subject of the influence of passivation/oxidation of the surface of the sample by air. Between grinding material and loading the sample into the reaction chamber, the crushed material of the sample (upper melted portion) $Ti_{30}Zr_{45}Ni_{25}$ was in the air for 7 days. After loading the sample into the reaction chamber, the chamber was evacuated to a pressure of $5 \cdot 10^{-6}$ bar. After the evacuation, hydrogen was introduced into the reaction chamber. The initial hydrogen pressure in the chamber was 268 kPa. As a result of the exposure of the sample at room temperature for 60 min, hydrogen uptake was not observed. During monotonous heating of the sample, active absorption of hydrogen by the sample began after reaching a temperature of 300 °C (Fig. 8). The active phase of hydrogen absorption continued to a temperature of about 400 °C. At a sample temperature above 450 °C, the absorption practically ceased. In the temperature range 300...400 °C, the sample absorbed about 0.95% by weight of hydrogen. Hydrogen evolution during thermal desorption from this sample occurred in the range 350...600 °C with max at 450 °C, which significantly differs from the kinetics of desorption of a hydrogen-saturated small particle at room temperature.



a



b

Fig. 7. Dependences of the temperature of the sample and heater (a), the pressure in the reaction chamber (b) on time upon re-saturation of the $Ti_{30}Zr_{45}Ni_{25}$ sample with hydrogen at room temperature

To confirm the obtained data, duplicate experiments on hydrogen sorption-desorption were carried out with a

Ti₃₀Zr₄₅Ni₂₅ sample in a setup with an MX7203 mass spectrometer. The sample was studied in the air for 7 days after grinding. Absorption at room temperature was not observed upon exposure to hydrogen for more than 2 h. Hydrogen sorption began only when heated above 200 °C. Active absorption took place in the range of 250...350 °C, plots of hydrogen sorption and thermal desorption after saturation of the samples with hydrogen are shown in Fig. 8.

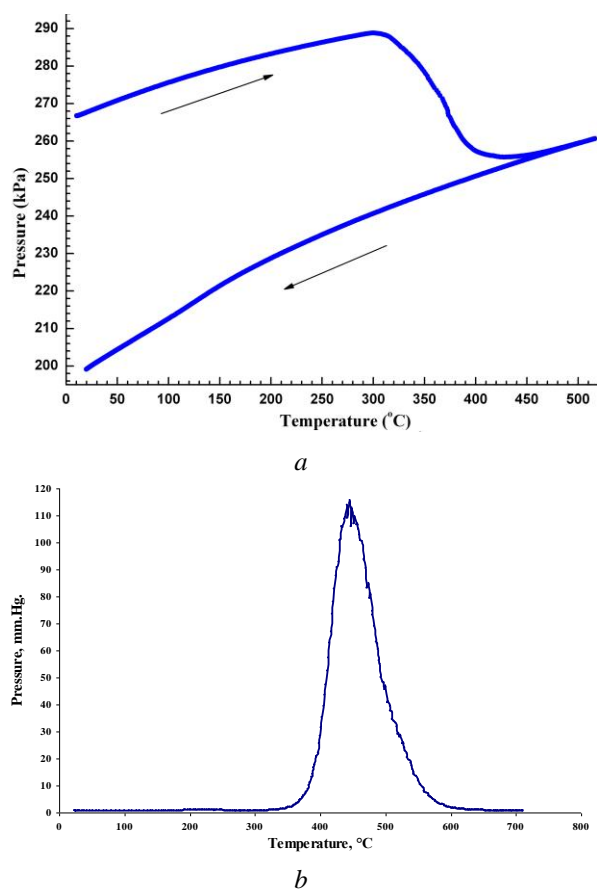


Fig. 8. Dependence of the pressure in the reaction chamber on the temperature of the Ti₃₀Zr₄₅Ni₂₅ sample (7 days in the air) for: sorption (a) and thermal desorption (b) of hydrogen

Thus, it can be argued that the presence of the ground Ti₃₀Zr₄₅Ni₂₅ sample in air leads to a gradual increase in the incubation period before the absorption of hydrogen at room temperature and subsequently completely eliminates this process. Nevertheless, the detected temperature ranges of sorption-desorption and the corresponding sorption capacity are unique for the Ti-Zr-Ni system and most other known metal hydride systems. This material can be an extremely promising hydrogen accumulator, research is ongoing.

CONCLUSION

The Ti₃₀Zr₄₅Ni₂₅ intermetallic material was synthesized using the hydride cycle technology with dehydrogenation of a portion of the (TiH₂)₃₀Zr₄₅Ni₂₅ sample by an electron beam in vacuum. The establishment of a stationary process of gradient heating of a sample by an electron beam made it possible to form a layered structure in the sample and fix all stages

of transformations, from the initial hydrides to the formation of a ternary alloy. Using scanning electron microscopy and X-ray diffraction analysis, it was established that under the influence of an electron beam, structural transformations occur in the sample, associated with the decay of titanium hydride and accompanied by a redistribution of hydrogen between the components of the sample. As a result of synthesis, the growth structures characteristic of the given system are formed in the sample, which are a mixture of (Ti,Zr)₂Ni phases, Laves phases C14 L-TiZrNi, α-(Ti,Zr). The study of hydrogen sorption and desorption processes by a synthesized sample showed that the structure of the sample formed upon heating by an electron beam promotes reversible absorption of hydrogen at room temperature up to 1.41 wt.% with heat evolution. Subsequent thermal desorption of hydrogen begins when the sample is heated above 40 °C. It was also found that after grinding a sample of Ti₃₀Zr₄₅Ni₂₅ and being in a ground state for more than 7 days in the air, the material loses its ability to absorb hydrogen at room temperature.

ACKNOWLEDGEMENTS

Authors thank gratefully to R. Vasilenko for the sample SEM/EDX investigations and I.V. Kolodiy for XRD investigations. Also, special thanks to M.M. Pylypenko and O.M. Bovda for the help in discussing the results.

REFERENCES

1. H.G. Hakobyan, A.G. Aleksanyan, S.K. Dolukhanyan, N.L. Mnatsakanyan. Zirconium intermetallides and their hydrides as obtained by the hydride cycle route // *International Journal of Self-Propagating High-Temperature Synthesis*. 2010, v. 19(1), p. 49-51.
2. S.K. Dolukhanyan, A.G. Aleksanyan, O.P. Ter-Galstyan, V.Sh. Shekhtman, M.K. Sakharov, G.E. Abrosimova. The peculiarities of the formation of alloys structure in the Ti-Zr-H system // *Chemical Physics*. 2007, v. 26 (11), p. 36-43.
3. S.K. Dolukhanyan, A.G. Aleksanyan, O.P. Ter-Galstyan, V.Sh. Shekhtman, M.K. Sakharov, G.E. Abrosimova. Specifics of the formation of alloys and their hydrides in the Ti-Zr-H system // *Russian Journal of Physical Chemistry B*. 2007, v. 2(6) p. 563-569.
4. S.K. Dolukhanyan, M.D. Nersesyan, A.B. Nalbandyan, I.P. Borovinskaya, A.G. Merzhanov. Combustion of transition metals in hydrogen // *Doc. USSR Academy of Sciences*. 1976, v. 231(3), p. 675-678.
5. S.K. Dolukhanyan, H.G. Hakobyan, and A.G. Aleksanyan. Combustion of metals in hydrogen and hydride production by self propagating high temperature synthesis // *Int. J. of SHS*. 1992, v. 1(4), p. 530-535.
6. A.G. Aleksanyan, D.G. Mayilyan, S.K. Dolukhanyan, V.Sh. Shekhtman, O.P. Ter-Galstyan. Synthesis of hydrides and production of alloys in the Ti-Hf-H system // *International journal Alternative Energy and Ecology*. 2008, v. 9(65), p. 22-26.
7. A.G. Aleksanyan, S.K. Dolukhanyan, A.A. Mantashanyan, D.G. Mayilyan, O.P. Ter-Galstyan, V.Sh.

She-khtman. A new technique for producing the alloys based on transition metals // *Carbon Nanomaterials in Clean Energy Hydrogen Systems. NATO Science Series*. 2008, p. 783-794.

8. S.K. Dolukhnyan, A.G. Aleksanyan, V.Sh. Shekhtman, A.A. Mantashanyan, D.G. Mayilyan, and O.P. Tergalastyan. A new method for producing alloys based on transition metals // *Chemical Journal of Armenia*. 2007, N 4(60), p. 545-569.

9. A. Kocjan, S. Kovacic, A. Gradisek, J. Kovac, P.J. McGuinness, T. Apih, J. Dolinsek, S. Kobe. Selective hydrogenation of Ti-Zr-Ni alloys // *International journal of hydrogen energy*. 2011, v. 36, p. 3056-3061.

10. M. Stroud, A.M. Viano, E.H. Majzoub, P.C. Gibbons, K.F. Kelton. Ti-Zr-Ni Quasicrystals: Structure and hydrogen // *Materials Research Society*. 1996, v. 400, p. 255-260.

11. R.M. Ribeiro, L.F. Lemus, D.S. dos Santos. Hydrogen absorption study of Ti-based alloys performed by melt-spinning // *Materials Research*. 2013, v. 16(3), p. 679-682.

12. Yu.P. Bobrov, O.M. Bovda, S.S. Grankin, O.E. Dmytrenko, L.V. Onishenko, O.S. Tortika. Hydrogen absorbing-desorbing behavior of melt-spun

Ti₃₀Zr₄₅Ni₂₅ alloy // *Metal physics and newest technologies. Special number*. 2008, v. 30, p. 329-336.

13. O.E. Dmytrenko, I.V. Kolodiy. Influence of the hydrogen saturation temperature on the structure of melt-spun Ti₃₀Zr₄₅Ni₂₅ alloy // *Problems of Atomic Science and Technology. Series "Vacuum, Pure Materials, Superconductors"*. 2018, N 1(113), p. 162-168.

14. O.E. Dmytrenko, O.E. Kozhevnikov, V.N. Pelykh. Application of electron-beam melting for refining nickel // *Problems of Atomic Science and Technology. Series "Vacuum, Pure Materials, Superconductors"*. 2003, N 5, p. 161-166.

15. O.M. Ivasin, D.G. Savvakina, N.M. Gumenyak. Dehydrogenation of titanium hydride powder and its role in sintering activation // *Metallophysics and latest technologies*. 2011, v. 33, N 7, p. 899-917.

16. D.G. Savvakina, N.M. Gumenyak. Synthesis of alloys based on the binary Zr-Ti system using dispersed zirconium hydride // *Metallophysics and latest technologies*. 2013, v. 35, N 3, p. 349-358.

17. O.M. Ivasishin, A.B. Bondarchuk, M.M. Gumenyak, D.G. Savvakina. Surface phenomenon upon heating of titanium hydride powder // *Physics and chemistry of solid-state*. 2011, v. 12, N 4, p. 900-907.

Статья поступила в редакцию 27.11.2019 г.

СИНТЕЗ МАТЕРИАЛОВ НАКОПИТЕЛЕЙ ВОДОРОДА В СИСТЕМЕ Ti-Zr-Ni ПО ТЕХНОЛОГИИ ГИДРИДНОГО ЦИКЛА ПРИ ДЕГИДРИРОВАНИИ ЭЛЕКТРОННЫМ ПУЧКОМ В ВАКУУМЕ

А.Е. Дмитренко, В.И. Дубинко, В.Н. Борисенко, К. Ирвин

Проведен синтез интерметаллического материала посредством дегидрирующего отжига образца (TiH₂)₃₀Zr₄₅Ni₂₅ в вакууме электронным пучком. Методом сканирующей электронной микроскопии и рентгеноструктурного анализа исследованы свойства полученного материала для установления структурно-фазового состава. Установлено, что длительное воздействие электронного пучка на образец, содержащий гидрид титана, приводит к ряду структурных превращений в материале, сопровождающихся перераспределением водорода из титана в цирконий и завершающихся синтезом тройного сплава с характерными структурами роста. Исследованы процессы сорбции-десорбции водорода синтезированным образцом, установлены температурные диапазоны данных процессов и поглотительная способность полученного материала. Показано, что сформировавшаяся при нагреве электронным пучком структура образца способствует поглощению водорода при комнатной температуре до 1,41 вес.%.

СИНТЕЗ МАТЕРІАЛІВ НАКОПИЧУВАЧІВ ВОДНЮ В СИСТЕМІ Ti-Zr-Ni ЗА ТЕХНОЛОГІЄЮ ГІДРИДНОГО ЦИКЛУ ПРИ ДЕГІДРУВАННІ ЕЛЕКТРОННИМ ПУЧКОМ У ВАКУУМІ

О.Е. Дмитренко, В.І. Дубінко, В.М. Борисенко, К. Ірвін

Проведено синтез інтерметалічного матеріалу за допомогою дегідруючого відпалу зразка (TiH₂)₃₀Zr₄₅Ni₂₅ у вакуумі електронним пучком. Методом скануючої електронної мікроскопії і рентгеноструктурного аналізу досліджені властивості отриманого матеріалу для встановлення структурно-фазового складу. Встановлено, що тривала дія електронного пучка на зразок, що містить гідрид титану, призводить до ряду структурних перетворень у матеріалі, що супроводжуються перерозподілом водню з титану в цирконій і завершуються синтезом потрійного сплаву з характерними структурами зростання. Досліджено процеси сорбції-десорбції водню синтезованим зразком, встановлені температурні діапазони даних процесів і поглинальна здатність отриманого матеріалу. Показано, що сформована при нагріванні електронним пучком структура зразка сприяє поглинанню водню при кімнатній температурі до 1,41 ваг.%.